

Spin States of Cobalt Ions in the Bulk and on the Surface of LaCoO₃ Probed by X-ray Absorption, Emission, and Photoelectron Spectra

V. R. Galakhov^{a,*}, M. S. Udintseva^a, D. A. Smirnov^b, A. A. Makarova^c, and K. Kuepper^d

^a Mikheev Institute of Metal Physics, Ural Branch, Russian Academy of Sciences, Yekaterinburg, 620108 Russia

^b Institute of Solid State and Material Physics, Dresden University of Technology, Dresden, 01062 Germany

^c Physikalische Chemie Institut für Chemie und Biochemie Freie Universität Berlin, Berlin, 14195 Germany

^d Department of Physics, University of Osnabrück, Osnabrück, 49076 Germany

*e-mail: galakhov@gmail.com

Received May 24, 2023; revised June 25, 2023; accepted June 26, 2023

We present X-ray photoelectron, Co $L_{2,3}$ and O K X-ray absorption, as well as Co $K\beta_{1,3}$ X-ray emission spectroscopy results of studies of the spin states of trivalent cobalt ions in single-crystal cobaltite LaCoO₃. We show that at room temperature, in the bulk of a LaCoO₃ single crystal, Co³⁺ ions are in the low-spin state, while high-spin Co²⁺, high-spin Co³⁺, low-spin Co³⁺, and probably also intermediate-spin Co³⁺ ions are located on the surface.

DOI: 10.1134/S0021364023601586

Lanthanum cobaltite, LaCoO₃, is a very interesting object from the point of view of studying spin states of Co³⁺ ions in it. In this compound Co³⁺ ions are octahedral surrounded by oxygen ions. It is known that trivalent cobalt ions ($3d^6$ electronic configuration) in a ligand field can be in low-spin (LS, $S = 0$), in intermediate spin (IS, $S = 1$), and in high-spin (HS, $S = 2$) configurations. At low temperatures (lower than 90 K), LaCoO₃ is a diamagnetic insulator with cobalt ions Co³⁺ in the low-spin state [1–4]. At temperatures above 90 K, LaCoO₃ goes into a paramagnetic state and at temperatures above 500 K, the metallic state is realized [1–4]. Attention of many researchers is focused on establishing the scenario of spin–spin transitions of trivalent cobalt ions in this compound.

The possibility of LS → IS transition was supported by the works [5–16]. The LS → IS scenario was rejected in favor of the LS → HS transition in [17–26]. At low temperatures, Co³⁺ ions should be in the low-spin state, but the authors of [27], based on the results of X-ray photoemission, suggested that Co³⁺ ions in LaCoO₃ at 100 K coexist in the LS, IS, and HS states. Using X-ray absorption Co $L_{2,3}$ spectra, the authors of [21] showed that at 20 K, the low-spin state of trivalent cobalt ions in LaCoO₃ is realized, and at 650 K, 50% of Co³⁺ ions are in the high-spin state, and 50% of ions are in the low-spin state.

Thus, the problem of spin states of cobalt ions in LaCoO₃ cobaltite at high temperatures has not yet been solved. Moreover, the question of spin states of Co³⁺ ions in LaCoO₃ at room temperature is still an open question. On the base of GGA + U calculations and photoelectron measurements, Pandey et al. [28] suggested the intermediate spin state of Co³⁺ ions in LaCoO₃. Based on the analysis of X-ray absorption Co $L_{2,3}$ spectra, it was assumed the low-spin character of Co³⁺ ions in LaCoO₃ at room temperature [29]. On the basis of measurements of O K X-ray absorption spectra, Suntivich et al. [30] confirmed the intermediate spin state on the surface of cobaltite and the low-spin state in the bulk. Therefore, the aim of our study is to determine spin states of Co³⁺ ions in LaCoO₃ at room temperature using complementary X-ray spectroscopy methods.

A single crystal of LaCoO₃ was grown by zone melting with radiation heating at the National Research Technological University MISiS (Moscow) in the group of Prof. Y.M. Mukovskii. X-ray diffraction was used to check the structural perfection and the single-phase nature of the sample. The elemental composition of the sample was checked using an JCSA-733 X-ray electron microanalyzer (JEOL). According to the X-ray microanalysis data, the composition of the sample is La_{0.98}Co_{1.00}O₃ (after converting mass % into atomic ones). It was not possible to determine the oxygen content with this equipment.

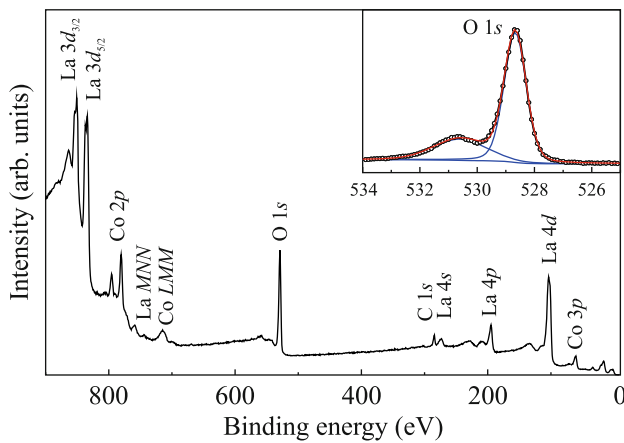


Fig. 1. (Color online) X-ray photoelectron survey and (inset) O 1s spectra of LaCoO₃.

X-ray photoelectron spectra were measured on a PHI6500 X-ray photoelectron spectrometer ci Multi-technique System using monochromatized Al $K\alpha$ radiation. In order to obtain a clean surface suitable for photoelectronic research, the single crystal was broken in a high vacuum chamber just before the measurements.

The cobalt $L_{2,3}$ and oxygen K X-ray absorption spectra were obtained at the Russian–German beam-line of the BESSY-II storage ring in total-photoelectron-yield mode using registration of the sample-drain current. To eliminate the influence of contamination of the parts of the spectrometer with oxygen-containing substances, the O K -edge spectra of the samples under study were normalized with respect to the oxygen spectrum obtained from a gold foil measured in the same energy range.

Co $K\beta$ emission spectra were measured at the BM20 synchrotron line of the European Synchrotron Radiation Center (ESRF, Grenoble) at room temperature and at 100 K.

Crystal-field multiplet calculations for high-spin and low-spin Co³⁺ ions were carried out using the CTM4XAS computer program taking into account the Coulomb and exchange interactions between $2p$ holes and $3d$ electrons, the splitting by the crystal field, spin–orbit interaction, and charge-transfer effects [31]. The crystal field parameters $10Dq$ were taken equal to 0.6 eV and 1.6 eV for high-spin and low-spin states of Co³⁺ ions in octahedra, respectively.

Figure 1 presents the survey X-ray photoelectron spectrum of LaCoO₃, which shows only signals from the elements included in the chemical formula. The 1s signal of carbon that appeared due to contamination of the sample surface is rather weak. The elemental composition of the sample determined by X-ray photoelectron analysis, La_{1.1}Co_{1.00}O_{3.5}, is close to that

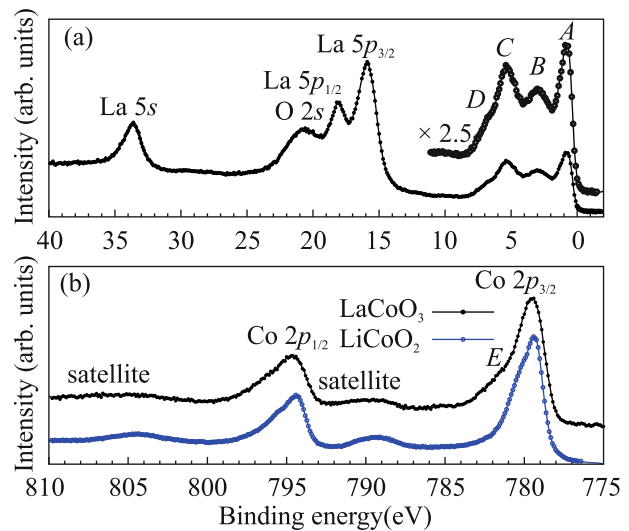


Fig. 2. (Color online) (a) X-ray photoelectron La 5s, O 2s, La 5p spectra, valence band spectrum of LaCoO₃ and (b) Co 2p spectra of LaCoO₃ and LiCoO₂.

obtained from our X-ray microanalysis measurements. The ratio between the amount of cobalt and lanthanum atoms corresponds to measurement errors. The somewhat overestimated oxygen content is apparently associated with the presence of OH hydroxyl on the surface of the sample. The manifestation of the signal from the hydroxyl group can be seen in the inset at the right of Fig. 1 which shows the O 1s X-ray photoelectron spectrum decomposed into two components. The intense peak at 528.8 eV is the O 1s state of bulk LaCoO₃. The high-energy component of the spectrum at 530.5 eV is due to OH hydroxyl. This spectrum is in good agreement with the literature spectra [32–34].

The valence-band X-ray photoelectron spectrum of LaCoO₃ is shown in Fig. 2a. In addition to the La 5s, La 5p, and O 2s signals, one can see features *A*, *B*, *C*, *D* in the region near the top of the valence band which are also previously noted in the literature [32–39]. According to the calculations in a cluster configuration–interaction model [33] and the LDA calculations of the density of electronic states [40], peak *A* stems from Co 3d states and also structure *C* and shoulder *D* have some Co 3d contribution whereas structure *B* is formed by O 2p states. Thus, our X-ray photoelectron studies of LaCoO₃ are consistent with the literature data. The electronic structure estimated from the photoelectron spectra corresponds to that of LaCoO₃.

Figure 2b shows Co $2p_{3/2,1/2}$ X-ray photoelectron spectra of LaCoO₃ and LiCoO₂. It is known that Co³⁺ ions in LiCoO₂ are in the low-spin state. The bands at binding energies of 790 and 804 eV are charge-transfer

satellites formed by the $\text{Co } 2p^5 3d^6$ final state of photoemission, while the main lines arise due to $\text{Co } 2p^5 3d^7 \underline{L}$ -states; here \underline{L} means the transfer of an electron from oxygen to cobalt. The spectra of LaCoO_3 and LiCoO_2 are close. Note, the spectrum of LaCoO_3 has shoulder E which can be explained either by the presence of Co^{2+} ions in the material [41–43] or by the nonlocal screening effect [44]. Note that nonlocal screening is impossible for low-spin states of Co^{3+} ions with fully occupied t_{2g}^6 orbitals [44]. Revealing the charge and spin states of ions in cobaltite will also clarify the nature of this shoulder in $\text{Co } 2p$ spectra of LaCoO_3 .

To determine the spin states of trivalent cobalt ions, we use the X-ray absorption $\text{Co } L$ spectra shown in the Fig. 3a. The spectra were measured at two orientations of the sample relative to the synchrotron beam: at almost perpendicular incidence of the beam (the angle between the crystal plane and the beam is 70° , spectrum 1) and at 40° (spectrum 2). The spectra show distinct features of A – B – C – D – E . Features A – B – C indicate the presence of Co^{2+} ions in the sample. This follows from the coincidence of the energy positions of these features with the peaks of the $\text{Co } L_3$ spectrum of CoO . In particular, feature A can serve as a “fingerprint” of Co^{2+} ions. This low-intensity prepeak structure associated with the admixture of divalent cobalt ions manifested itself in complex cobaltites: in cobalt-based heterostructures and in layered cobaltites $\text{LnBaCo}_2\text{O}_{6-\delta}$ [45, 46], as well as after plastic deformation of cobaltites [47]. Divalent cobalt ions appear in the material due to a slight oxygen deficiency or due to the reduction of trivalent cobalt ions on the surface [48].

The theoretical spectra calculated for HS-Co^{3+} and HS-Co^{2+} ions are shown in the lower part of Fig. 3a. The HS states of Co^{3+} ions are displayed in the energy region 778–779 eV of the spectrum (B – C features). Feature C has contributions from both HS-Co^{3+} and HS-Co^{2+} ions and feature E is a characteristic of LS-Co^{3+} ions.

Let us try to extract the spectral signals of trivalent cobalt ions. It is obvious that the spectrum measured for the sample placed at the small angle between the surface of the crystal and the synchrotron beam is determined to a greater extent by the surface than the spectrum obtained with an almost perpendicular beam incidence on the plane of the sample.

In Fig. 3a, the two $\text{Co } L_3$ spectra of LaCoO_3 are plotted at the same intensity of feature A . Normalization to the A peak assumes an equal contribution of Co^{2+} ions to the formation of these spectra. The applied spectrum registration geometry makes it possible to compensate for the contribution of signals from surface layers. It can be assumed that the ions

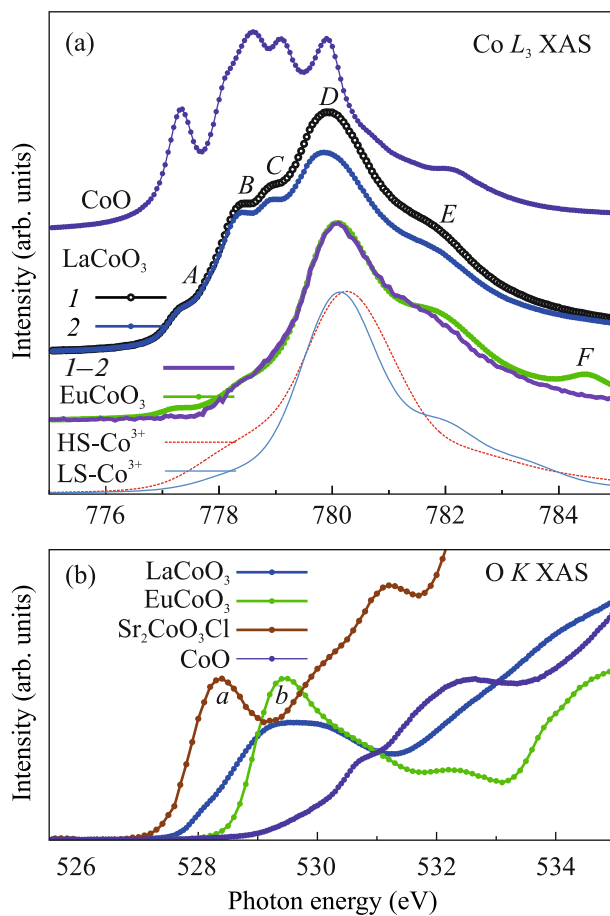


Fig. 3. (Color online) (a) $\text{Co } L_3$ X-ray absorption spectra of single crystalline CoO and LaCoO_3 . The spectra of LaCoO_3 are measured at two orientations of the sample with respect to the synchrotron beam: at nearly perpendicular beam incidence (an angle between the plane of the crystal of 70° , spectrum 1) and at an angle of 40° between the plane of the crystal and the beam (spectrum 2); (1–2) difference spectrum. In order to compare with the spectrum of EuCoO_3 (LS-Co^{3+} ions), the difference spectrum is increased by a factor of 4.7. The results of a multiplet calculation of the spectra of Co^{3+} ions in the high-spin (HS) and low-spin (LS) states in an octahedral environment are presented. (b) $\text{O } K$ X-ray absorption spectra of LaCoO_3 , EuCoO_3 , $\text{Sr}_2\text{CoO}_3\text{Cl}$, and CoO .

HS-Co^{2+} , HS-Co^{3+} and LS-Co^{3+} and, possibly, IS-Co^{3+} .

The difference spectrum obtained with this ratio of spectral intensities characterizes the Co^{3+} ions in the LaCoO_3 volume. It practically coincides with the spectrum of cobaltite EuCoO_3 , in which Co^{3+} ions are in the low-spin state [49], and with the theoretical spectrum for LS-Co^{3+} ions. The F feature in the spectrum of EuCoO_3 is the $\text{Ba } M_5$ line, which appeared due to the contamination of the sample with a barium impurity during synthesis. It follows from these exper-

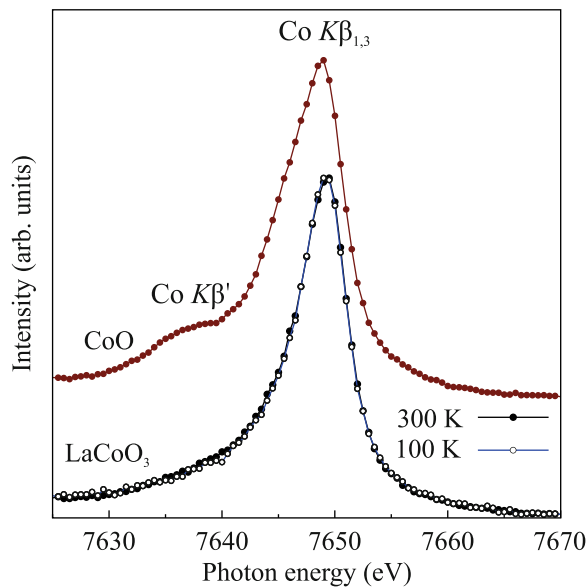


Fig. 4. (Color online) Co $K\beta$ X-ray emission spectra of CoO and LaCoO₃ single crystals. The spectra of LaCoO₃ were measured at room temperature and at about 100 K.

iments that the Co³⁺ ions in the bulk of LaCoO₃ at room temperature are in the low-spin state. This is in agreement with the results of [29], in which a similar conclusion was made based on an analysis of the shape of absorption Co $L_{2,3}$ spectra.

A somewhat different result follows from measurements of O K X-ray absorption. Figure 3b shows the O K X-ray absorption spectra of LaCoO₃, EuCoO₃, Sr₂CoO₃Cl, and CoO. These spectra are related to the O $1s \rightarrow O 2p$ electron transition. Since the electronic orbitals of cobalt and oxygen are hybridized, the O K X-ray absorption spectrum reflects the distribution of unoccupied Co $3d$ (t_{2g} and e_g) states.

Cobalt ions in the pyramids of Sr₂CoO₃Cl were established to be in the HS-state [50]. The first maximum of the spectrum (a) should be described to the empty Co $3d_{xz}$, $3d_{yz}$, and $3d_{xy}$ orbitals. Co³⁺ ions in octahedra of EuCoO₃ are known to be in the low-spin state [49]. The t_{2g} shell is completely occupied. It does not appear in the absorption spectrum. Peak b in the O K spectrum reflects unoccupied e_g states. The spectrum of CoO is much higher in energy and almost does not cover the states of trivalent cobalt ions. The spectrum of LaCoO₃ is much broader than the spectrum of EuCoO₃ and extends into the low-energy area. It means that the t_{2g} states in LaCoO₃ are partially empty.

There is a significant discrepancy between the results of measuring the L spectra of cobalt and the K spectra of oxygen, which can be explained by the

difference between the states of Co $3d$ on the surface and in the bulk of the sample. Since the X-ray absorption spectra were measured in the surface-sensitive total-electron-yield mode, the depth of analysis is about 5–10 nm. Due to the orientation of the single crystal relative to the synchrotron beam, cobalt spectra were used to distinguish the Co $3d$ states in the bulk. On the other hand, the oxygen spectrum reflects the electronic states both in the bulk and on the surface. Unlike the cobalt spectra, these contributions were not separated. Thus, it follows from measurements of the O K spectra that on the surface of the LaCoO₃ single crystal, the Co³⁺ ions are in a mixture of the LS and HS states and, possibly, the IS state. The surface also contains high spin Co²⁺ ions, which were detected using Co L spectra.

The spin states of cobalt ions can be efficiently estimated from Co $K\beta$ X-ray emission spectra ($3p \rightarrow 1s$ electron transition). Due to the exchange interaction between the $3p$ hole and $3d$ electrons in the final state of the emission process, these spectra are sensitive to the spin state of $3d$ electrons (see, for example, [51–54]). In the presence of a nonzero spin of a system of $3d$ -electrons, the $K\beta$ -spectrum is split into a rather narrow $K\beta_{1,3}$ -line and a wide low-energy satellite $K\beta'$, the intensity ratio of the satellite (I') to the main line (I) is determined by the total spin of $3d$ electrons: $I'/I = S/(S+1)$. Here S is the total spin of $3d$ electrons. The energy difference between the $K\beta_{1,3}$ and $K\beta'$ lines is proportional to $(2S+1)$ (in the case if $S \neq 0$; for $S = 0$ the energy difference is equal to 0).

Figure 4 shows the Co $K\beta$ spectra of LaCoO₃ measured at room temperature and at about 100 K. For comparison, the spectrum of CoO is presented (high spin Co²⁺ ions, $S = 3/2$). The spectra of LaCoO₃ do not contain a satellite characterized systems with nonzero spin of $3d$ electrons. Moreover, an increase in temperature from 100 K to room temperature practically does not change the spectrum. Fluorescent radiation was excited by a synchrotron beam; therefore, the results obtained should be referred to the bulk of the sample. Thus, this experiment confirms the low-spin state of trivalent cobalt ions in the bulk of LaCoO₃.

To summarize, we have carried out characterization of single-crystalline cobaltite LaCoO₃ by X-ray spectroscopy methods. We have established that Co³⁺-ions in the bulk of single-crystalline LaCoO₃ at room temperature are in the low spin state. On the surface of LaCoO₃, there is a mixture of HS-Co²⁺, HS-Co³⁺, IS-Co³⁺ and LS-Co³⁺ ions.

ACKNOWLEDGMENTS

We thank Prof. K.O. Kvashnina (European Synchrotron, Grenoble, France) and Dr. V.V. Mesilov (Yale-NUS College, Singapore) for their assistance in measurements of X-ray emission Co *K* spectra on the BM20 line (ESRF, Grenoble, project HC-2890). We acknowledge the European Synchrotron Radiation Facility for provision of synchrotron radiation facilities. The X-ray spectra were measured with partial financial support from Bilateral Program “Russian–German Laboratory at BESSY.”

FUNDING

The work was supported by the Ministry of Science and Higher Education of the Russian Federation (project no. 122021000039-4, theme Electron, state assignment for the Mikheev Institute of Metal Physics).

CONFLICT OF INTEREST

The authors declare that they have no conflicts of interest.

OPEN ACCESS

This article is licensed under a Creative Commons Attribution 4.0 International License, which permits use, sharing, adaptation, distribution and reproduction in any medium or format, as long as you give appropriate credit to the original author(s) and the source, provide a link to the Creative Commons license, and indicate if changes were made. The images or other third party material in this article are included in the article’s Creative Commons license, unless indicated otherwise in a credit line to the material. If material is not included in the article’s Creative Commons license and your intended use is not permitted by statutory regulation or exceeds the permitted use, you will need to obtain permission directly from the copyright holder. To view a copy of this license, visit <http://creativecommons.org/licenses/by/4.0/>.

REFERENCES

1. G. Jonker and J. V. Santen, *Physica* (Amsterdam, Neth.) **19**, 120 (1953).
2. P. M. Raccah and J. B. Goodenough, *Phys. Rev.* **155**, 932 (1967).
3. G. Thornton, B. Tofield, and D. Williams, *Solid State Commun.* **44**, 1213 (1982).
4. S. R. English, J. Wu, and C. Leighton, *Phys. Rev. B* **65**, 220407 (2002).
5. M. A. Korotin, S. Y. Ezhov, I. V. Solovyev, V. I. Anisimov, D. I. Khomskii, and G. A. Sawatzky, *Phys. Rev. B* **54**, 5309 (1996).
6. S. Yamaguchi, Y. Okimoto, and Y. Tokura, *Phys. Rev. B* **55**, R8666 (1997).
7. P. G. Radaelli and S.-W. Cheong, *Phys. Rev. B* **66**, 094408 (2002).
8. I. A. Nekrasov, S. V. Streltsov, M. A. Korotin, and V. I. Anisimov, *Phys. Rev. B* **63**, 235113 (2003).
9. G. Maris, Y. Ren, V. Volotchaev, C. Zobel, T. Lorenz, and T. T. M. Palstra, *Phys. Rev. B* **67**, 224423 (2003).
10. M. Magnuson, S. M. Butorin, C. S  the, J. Nordgren, and P. Ravindran, *Europhys. Lett.* **68**, 289 (2004).
11. D. Phelan, D. Louca, S. Rosenkranz, S.-H. Lee, Y. Qiu, P. J. Chupas, R. Osborn, H. Zheng, J. F. Mitchell, J. R. D. Copley, J. L. Sarrao, and Y. Moritomo, *Phys. Rev. Lett.* **96**, 027201 (2006).
12. G. Vank  , J.-P. Rueff, A. Mattila, Z. N  meth, and A. Shukla, *Phys. Rev. B* **73**, 024424 (2006).
13. R. F. Klie, J. C. Zheng, Y. Zhu, M. Varela, J. Wu, and C. Leighton, *Phys. Rev. Lett.* **99**, 047203 (2007).
14. V. V. Sikolenko, S. L. Molodtsov, M. Izquierdo, I. O. Troyanchuk, D. Karpinsky, S. I. Tiutiunnikov, E. Efimova, D. Prabhakaran, D. Novoselov, and V. Efimov, *Phys. B (Amsterdam, Neth.)* **536**, 597 (2018).
15. V. V. Sikolenko, I. O. Troyanchuk, D. V. Karpinsky, A. Rogalev, F. Wilhelm, R. Rosenberg, D. Prabhakaran, E. A. Efimova, V. V. Efimov, S. I. Tiutiunnikov, and I. A. Bobrikov, *Phys. Solid State* **60**, 288 (2018).
16. M. Feygenson, D. Novoselov, S. Pascarelli, R. Chernikov, O. Zaharko, F. Porcher, D. Karpinsky, A. Nikitin, D. Prabhakaran, A. Sazonov, and V. Sikolenko, *Phys. Rev. B* **100**, 054306 (2019).
17. M. Zhuang, W. Zhang, and N. Ming, *Phys. Rev. B* **57**, 10705 (1998).
18. S. Noguchi, S. Kawamata, K. Okuda, H. Nojiri, and M. Motokawa, *Phys. Rev. B* **66**, 094404 (2002).
19. K. Kn  zek, J. Hejtm  nek, and P. Nov  k, *J. Phys.: Condens. Matter* **18**, 3285 (2006).
20. A. Podlesnyak, S. Streule, J. Mesot, M. Medarde, E. Pomjakushina, K. Conder, A. Tanaka, M. W. Haverkort, and D. I. Khomskii, *Phys. Rev. Lett.* **97**, 247208 (2006).
21. M. W. Haverkort, Z. Hu, J. C. Cezar, T. Burnus, H. Hartmann, M. Reuther, C. Zobel, T. Lorenz, A. Tanaka, N. B. Brookes, H. H. Hsieh, H.-J. Lin, C. T. Chen, and L. H. Tjeng, *Phys. Rev. Lett.* **97**, 176405 (2006).
22. M. Medarde, C. Dallera, M. Grioni, J. Voigt, A. Podlesnyak, E. Pomjakushina, K. Conder, T. Neisius, O. Tjernberg, and S. N. Barilo, *Phys. Rev. B* **73**, 054424 (2006).
23. N. Sundaram, Y. Jiang, I. E. Anderson, D. P. Belanger, C. H. Booth, F. Bridges, J. F. Mitchell, T. Proffen, and H. Zheng, *Phys. Rev. Lett.* **102**, 026401 (2009).
24. K. Kn  zek, J. Hejtm  nek, Z. Jir  k, P. Tomeš, P. Henry, and A. Andr  , *Phys. Rev. B* **79**, 134103 (2009).
25. V. Kr  pek, P. Nov  k, J. Kuneš, D. Novoselov, D. M. Korotin, and V. I. Anisimov, *Phys. Rev. B* **86**, 195104 (2012).
26. R. Yu. Babkin, K. V. Lamonova, S. M. Orel, S. G. Ovchinnikov, and Yu. G. Pashkevich, *JETP Lett.* **99**, 476 (2014).
27. S. R. Barman and D. D. Sarma, *Phys. Rev. B* **49**, 13979 (1994).
28. S. K. Pandey, A. Kumar, S. Patil, V. R. R. Medicherla, R. S. Singh, K. Maiti, D. Prabhakaran, A. T. Boothroyd, and A. V. Pimpale, *Phys. Rev. B* **77**, 045123 (2008).

29. Z. Shen, M. Qu, J. Shi, F. E. Oropeza, V. A. de la Pena O'Shea, G. Gorni, C. Tian, J. P. Hofmann, J. Cheng, J. Li, and K. H. Zhang, *J. Energy Chem.* **65**, 637 (2022).
30. J. Suntivich, W. T. Hong, Y.-L. Lee, J. M. Rondinelli, W. Yang, J. B. Goodenough, B. Dabrowski, J. W. Freeland, and Y. Shao-Horn, *J. Phys. Chem. C* **118**, 1856 (2014).
31. E. Stavitski and F. M. F. de Groot, *Micron* **41**, 687 (2010).
32. R. P. Vasquez, *Phys. Rev. B* **54**, 14938 (1996).
33. T. Saitoh, T. Mizokawa, A. Fujimori, M. Abbate, Y. Takeda, and M. Takano, *Phys. Rev. B* **55**, 4257 (1997).
34. K. A. Stoerzinger, W. T. Hong, E. J. Crumlin, H. Bluhm, M. D. Biegalski, and Y. Shao-Horn, *J. Phys. Chem. C* **118**, 19733 (2014).
35. B. W. Veal and D. J. Lam, *J. Appl. Phys.* **49**, 1461 (1978).
36. L. Richter, S. D. Bader, and M. B. Brodsky, *Phys. Rev. B* **22**, 3059 (1980).
37. J. Kemp, D. Beal, and P. Cox, *J. Solid State Chem.* **86**, 50 (1990).
38. M. Abbate, J. C. Fuggle, A. Fujimori, L. H. Tjeng, R. P. C. T. Chen, G. A. Sawatzky, H. Eisaki, and S. Uchida, *Phys. Rev. B* **47**, 16124 (1993).
39. L. Heymann, M. L. Weber, M. Wohlgemuth, M. Risch, R. Dittmann, C. Baeumer, and F. Gunkel, *ACS Appl. Mater. Interfaces* **14**, 14129 (2022).
40. D. Takegami, L. Nicola, T. C. Koethe, D. Kasinathan, C. Y. Kuo, Y. F. Liao, K. D. Tsuei, G. Panaccione, F. Offi, G. Monaco, N. B. Brookes, J. Minár, and L. H. Tjeng, *Phys. Rev. B* **99**, 165101 (2019).
41. T. Y. Ma, S. Dai, M. Jaroniec, and S. Z. Qiao, *J. Am. Chem. Soc.* **136**, 13925 (2014).
42. L. Xu, Q. Jiang, Z. Xiao, X. Li, J. Huo, S. Wang, and L. Dai, *Angew. Chem. Int. Ed. Engl.* **55**, 5277 (2016).
43. Y. Liu, X. Kong, X. Guo, Q. Li, J. Ke, R. Wang, Q. Li, Z. Geng, and J. Zeng, *ACS Catal.* **10**, 1077 (2020).
44. A. Hariki, A. Yamanaka, and T. Uozumi, *Phys. Soc. Jpn.* **84**, 073706 (2015).
45. S. L. Wachowski, I. Szpunar, M. H. Sørby, A. Mielewczyk-Gryń, M. Balaguer, C. Ghica, M. C. Istrate, M. Gazda, A. E. Gunnæs, J. M. Serra, T. Norby, and R. Strandbakke, *Acta Mater.* **199**, 297 (2020).
46. I. Szpunar, R. Strandbakke, M. H. Sørby, S. L. Wachowski, M. Balaguer, M. Tarach, J. Serra, A. Witkowska, E. Dzik, T. Norby, M. Gazda, and A. Mielewczyk-Gryń, *Materials* **13**, 4044 (2020).
47. V. R. Galakhov, M. S. Udintseva, S. V. Naumov, S. N. Shamin, and B. A. Gizhevskii, *JETP Lett.* **116**, 367 (2022).
48. M. García-Fernández, V. Scagnoli, U. Staub, A. M. Mulders, M. Janousch, Y. Bodenthin, D. Meister, B. D. Patterson, A. Mirone, Y. Tanaka, T. Nakamura, S. Grenier, Y. Huang, and K. Conder, *Phys. Rev. B* **78**, 054424 (2008).
49. Z. Hu, H. Wu, M. W. Haverkort, H. H. Hsieh, H. J. Lin, T. Lorenz, J. Baier, A. Reichl, I. Bonn, C. Felser, A. Tanaka, C. T. Chen, and L. H. Tjeng, *Phys. Rev. Lett.* **92**, 207402 (2004).
50. C. S. Knee, D. J. Price, M. R. Lees, and M. T. Weller, *Phys. Rev. B* **68**, 174407 (2003).
51. J.-P. Rueff, C.-C. Kao, V. V. Struzhkin, J. Badro, J. Shu, R. J. Hemley, and H. K. Mao, *Phys. Rev. Lett.* **82**, 3284 (1999).
52. G. Vankó, T. Neisius, G. Molnár, F. Renz, S. Kárpáti, A. Shukla, and F. M. F. de Groot, *J. Phys. Chem. B* **110**, 11647 (2006).
53. J. Herrero-Martín, J. L. García-Munoz, K. Kvashnina, E. Gallo, G. Subías, J. A. Alonso, and A. J. Barón-González, *Phys. Rev. B* **86**, 125106 (2012).
54. J.-M. Chen, Y.-Y. Chin, M. Valldor, Z. Hu, J.-M. Lee, S.-C. Haw, N. Hiraoka, H. Ishii, C.-W. Pao, K.-D. Tsuei, J.-F. Lee, H.-J. Lin, L.-Y. Jang, A. Tanaka, C.-T. Chen, and L. H. Tjeng, *J. Am. Chem. Soc.* **136**, 1514 (2014).